Precision measurement of the Ξ_b^0 baryon lifetime

R. Aaij *et al.*[*]
(LHCb Collaboration)

(Received 16 July 2025; accepted 27 August 2025; published 29 September 2025)

A sample of pp collision data, corresponding to an integrated luminosity of 5.4 fb^{-1} and collected by the LHCb experiment during LHC Run 2, is used to measure the ratio of the lifetime of the Ξ_b^0 baryon to that of the Λ_b^0 baryon, $r_\tau \equiv \tau_{\Xi_b^0}/\tau_{\Lambda_b^0}$. The value $r_\tau^{\mathrm{Run}\,2} = 1.004 \pm 0.009 \pm 0.006$ is obtained, where the first uncertainty is statistical and the second systematic. This value is averaged with the corresponding value from Run 1 to obtain $r_\tau = 1.004 \pm 0.008 \pm 0.005$. Multiplying by the known value of the Λ_b^0 lifetime yields $\tau_{\Xi_b^0} = 1.475 \pm 0.012 \pm 0.008 \pm 0.009$ ps, where the last uncertainty is due to the limited knowledge of the Λ_b^0 lifetime. This measurement improves the precision of the current world average of the Ξ_b^0 lifetime by about a factor of two, and is in good agreement with the most recent theoretical predictions.

DOI: 10.1103/sllb-p3j8

I. INTRODUCTION

The heavy-quark expansion (HQE) [1] is a theoretical framework that predicts the inclusive decay rates of beauty hadrons through an expansion in powers of the strong coupling constant, α_s, and $\Lambda_{\mathrm{QCD}}/m_b$. Here, Λ_{QCD} is the energy scale at which the strong-interaction coupling becomes large, $\mathcal{O}(100\ \mathrm{MeV})$, and m_b is the b-quark mass. When combined with precise measurements of heavy-quark decays, the HQE framework can be used to calculate b-hadron parameters required for the determination of Cabibbo-Kobayashi-Maskawa [2] matrix elements, which in turn provide constraints on physics beyond the Standard Model.

A stringent test of the HQE framework is to confront its predictions for the total decay widths Γ of various b hadrons with precise measurements of the corresponding lifetimes, $\tau = \hbar/\Gamma$. Here, b hadron refers to a baryon (meson) containing a single b quark and any pair of u, d or s quarks (a single $\bar{u}$, $\bar{d}$, or $\bar{s}$ antiquark). At leading order within the HQE framework, the decay width of all b hadrons is equal to that of the free b quark. Higher-order corrections account for nonperturbative effects, which are described by the kinetic, Darwin and chromomagnetic operators [3–6], as well as interactions of the b quark with the light valence quarks. It is in the interactions of the b quark with the light valence quarks that significant differences in b-hadron lifetimes emerge. The beauty baryons, $\Lambda_b^0(bud)$, $\Xi_b^0(bus)$, $\Xi_b^-(bds)$, and $\Omega_b^-(bss)$ have different pairs of light quarks, and thus the measurement of their lifetimes probes the effects of the light valence quark contributions on their total decay widths.

A recent precise measurement of the lifetime ratio $\tau_{\Xi_b^-}/\tau_{\Lambda_b^0} = 1.078 \pm 0.012 \pm 0.007$ [7] shows that the light valence quark effects result in a difference of about 8% in the total decay widths of the Λ_b^0 and Ξ_b^- baryons, which is in good agreement with the HQE prediction [3]. The only measurement of the Ξ_b^0 baryon lifetime has been performed by the LHCb collaboration using data samples corresponding to an integrated luminosity of 3 fb^{-1} collected at $\sqrt{s} = 7$ and 8 TeV (Run 1). The value of the lifetime ratio $\tau_{\Xi_b^0}/\tau_{\Lambda_b^0} = 1.006 \pm 0.018 \pm 0.010$ [8] is reported, which is consistent with the HQE prediction.

In this paper, a new measurement of the Ξ_b^0 baryon lifetime is reported using a pp collision data sample collected between 2016 and 2018 (Run 2) by the LHCb experiment at $\sqrt{s} = 13$ TeV, corresponding to an integrated luminosity of 5.4 fb^{-1}. The integrated luminosity and $b\bar{b}$ production cross-section are both about a factor of two larger compared to the previous analysis [8]. The lifetime ratio $\tau_{\Xi_b^0}/\tau_{\Lambda_b^0}$ is measured using the decays $\Xi_b^0 \to \Xi_c^+\pi^-$ and $\Lambda_b^0 \to \Lambda_c^+\pi^-$, where both the Ξ_c^+ and Λ_c^+ baryons are reconstructed in the $pK^-\pi^+$ final state. Although the $\Xi_c^+ \to pK^-\pi^+$ decay is Cabibbo-suppressed, the chosen Ξ_b^0 decay mode provides the largest signal yield per unit luminosity in LHCb due to the relatively low multiplicity and the absence of long-lived hyperons in the final state.[1]

[*]Full author list given at the end of the article.

[1]The inclusion of charge-conjugate processes is implied throughout.

The quantity that is measured experimentally is the ratio of efficiency-corrected signal yields as a function of the decay time, t,

$$R(t) \equiv \frac{N[\Xi_b^0 \to \Xi_c^+\pi^-](t)}{N[\Lambda_b^0 \to \Lambda_c^+\pi^-](t)} \cdot \frac{\varepsilon[\Lambda_b^0 \to \Lambda_c^+\pi^-](t)}{\varepsilon[\Xi_b^0 \to \Xi_c^+\pi^-](t)} = R_0 \exp(\lambda t), \tag{1}$$

where R_0 is an overall normalization factor, and N and ε represent the signal yields and efficiencies, respectively, of the decay mode indicated inside the brackets. The parameter λ is related to the lifetimes of the Λ_b^0 and Ξ_b^0 baryons through

$$\lambda \equiv \frac{1}{\tau_{\Lambda_b^0}} - \frac{1}{\tau_{\Xi_b^0}}. \tag{2}$$

The ratio of lifetimes is then

$$r_\tau \equiv \frac{\tau_{\Xi_b^0}}{\tau_{\Lambda_b^0}} = \frac{1}{1 - \lambda\tau_{\Lambda_b^0}}. \tag{3}$$

II. DETECTOR AND SIMULATION

The LHCb detector [9,10] is a single-arm forward spectrometer covering the pseudorapidity range $2 < \eta < 5$, designed for the study of particles containing b or c quarks. The detector used for this analysis includes a high-precision tracking system consisting of a silicon-strip vertex detector surrounding the pp interaction region [11], a large-area silicon-strip detector located upstream of a dipole magnet with a bending power of about 4 T m, and three stations of silicon-strip detectors and straw drift tubes [12] placed downstream of the magnet. The tracking system provides a measurement of the momentum, p, of charged particles with a relative uncertainty that varies from 0.5% at low momentum to 1.0% at 200 GeV/c. The polarity of the LHCb magnet is alternated regularly throughout each period of data taking. The minimum distance of a track to a primary pp collision vertex (PV), the impact parameter (IP), is measured with a resolution of approximately $\sigma_{\mathrm{IP}} = (15 + 29/p_{\mathrm{T}})$ μm, where p_{T} is the component of the momentum transverse to the beam, in GeV/c. Different types of charged hadrons are distinguished using information from two ring-imaging Cherenkov detectors [13]. Photons, electrons and hadrons are identified by a calorimeter system consisting of scintillating-pad and preshower detectors, an electromagnetic and a hadronic calorimeter. Muons are identified by a system composed of alternating layers of iron and multiwire proportional chambers [14]. The online event selection is performed by a trigger [15], which consists of a hardware stage (L0), based on information from the calorimeter and muon systems, followed by a software stage, which applies a full event reconstruction. The software stage employs a multivariate algorithm [16,17] to identify secondary vertices consistent with the decay of a b hadron.

Simulation is required to model the effects of the detector acceptance and the imposed selection requirements. In the simulation, pp collisions are generated using PYTHIA [18] with a specific LHCb configuration [19]. Decays of unstable particles are described by EvtGen [20], in which final-state radiation is generated using PHOTOS [21]. The interaction of the generated particles with the detector, and its response, are implemented using the GEANT4 toolkit [22] as described in Ref. [23]. The underlying pp interaction is reused multiple times, with an independently generated signal decay each time [24]. Simulated $\Xi_b^0 \to \Xi_c^+\pi^-$ and $\Lambda_b^0 \to \Lambda_c^+\pi^-$ decays are generated separately for each of the three data-taking years: 2016, 2017, and 2018. The simulation reflects the running conditions specific to each year. These conditions mainly account for adjustments in the hardware and software trigger thresholds, which are modified to accommodate variations in the instantaneous luminosity.

III. CANDIDATE SELECTION

Signal Ξ_b^0 (Λ_b^0) candidates are formed by fitting a $\Xi_c^+ \to pK^-\pi^+$ ($\Lambda_c^+ \to pK^-\pi^+$) candidate decay with a π^- candidate to a common vertex. Hereafter, the notation H_b and H_c refers to the b and c baryons. All final-state particles from the H_b baryons are required to have trajectories that are significantly detached from all PVs in the event, characterized by the quantity χ^2_{IP}, which is defined as the difference in the vertex-fit χ^2 of a given PV reconstructed with and without the particle in question. The final-state hadrons are also required to have particle identification (PID) responses that are consistent with the decay hypothesis. The H_c candidates are required to be well separated from all PVs in the event, have good decay-vertex fit quality, and have mass, $M(pK^-\pi^+)$, within 15 MeV/c^2 (25 MeV/c^2) of the known Ξ_c^+ (Λ_c^+) baryon mass $m_{\Xi_c^+}$ ($m_{\Lambda_c^+}$) [25], which corresponds to about 2.5 (3.5) times the mass resolution. The H_c decay time must satisfy $-0.2 < t_{\Xi_c^+} < 5.0$ ps ($-0.5 < t_{\Lambda_c^+} < 2.5$ ps), where the lower bound accounts for the decay-time resolution, and the upper bound is approximately ten times the known lifetime [25]. The decay time of the H_c (H_b) baryon is obtained using $t = d\frac{M}{p}$, where d, M and p are the measured decay length, mass and total momentum of the H_c (H_b) baryon. The H_b decay vertex is required to have a good fit quality and be well separated from all PVs in the event. The PV with the smallest χ^2_{IP} is assigned as the production point of the H_b candidate from which the decay time is measured.

Mass vetoes, in combination with additional PID requirements, are used to suppress cross-feeds from misidentified $D^+_{(s)} \to K^+K^-\pi^+$, $D^{*+} \to D^0(K^+K^-)\pi^+$, and

$D^+ \to K^-\pi^+\pi^+$ decays mimicking $\Lambda_c^+ \to pK^-\pi^+$ decays, as well as $\phi \to K^+K^-$ decays in which a K^+ meson is misidentified as a proton. These vetoes reduce the background in the Λ_b^0 and Ξ_b^0 samples by approximately 12% each, while retaining about 98.5% of the signal.

Signal H_b candidates are divided into two subsamples based on the association of specific hardware triggers with reconstructed particles. The first category, "triggered on signal" (TOS), contains those candidates in which one or more of the final-state hadrons from the signal decay are associated with a positive L0 trigger decision from the calorimeter. The second category, "triggered independently of the signal" (TIS), represents the case where a positive L0 trigger decision is due to other particles in the event [26]. For a given event, both the TOS and TIS requirements may be satisfied, in which case the event is classified as TOS. The TOS candidates tend to have larger p_{T} than the TIS candidates due to the high energy transverse to the beamline that is required by the hadron trigger. Signal candidates are required to be in one of these two categories, which comprises 96% of the H_b signal decays selected by any L0 trigger in the data. At the level of the software trigger, the signal candidates are required to satisfy the requirements of the topological trigger, detailed in Refs. [16,17].

A. Simulation corrections

A set of weights and corrections are applied to the simulation to account for imperfect modeling of the signal decays and the detector response. The weights that are applied to the simulation correct for the H_c decay kinematics, the Λ_b^0 baryon lifetime, the (p_{T}, η) spectra of the H_b baryons and the fractions of TOS and TIS events. Weights to account for differences in the H_c decay kinematics are obtained from the ratio of the two-dimensional mass distributions of $M(pK^-)$ versus $M(K^-\pi^+)$ in background-subtracted data relative to those obtained from simulation samples. The Λ_b^0 lifetime weight accounts for a small difference between the value of $\tau_{\Lambda_b^0}$ used in the simulation (1.451 ps) and the known value of 1.468 ps [25]. The (p_{T}, η) weights (w_{kin}) for H_b are obtained by taking the ratio of the background-subtracted signal distributions in data to the corresponding distributions in simulation, separately for each L0 trigger category. Lastly, TIS/TOS weights are then applied to the simulation so that the fractions of TOS and TIS events match those in the data. The p_{T} and η spectra of background-subtracted data [27] and simulation with and without the kinematic weights are compared in Fig. 1, showing improved agreement between the data and simulation after the correction is applied.

In addition to the weights, a correction is applied to the 2017 and 2018 simulations to account for differences in the IP resolution and in the χ^2 distributions from the vertex fit between data and simulation, as described in Ref. [7]. Small adjustments are made to the χ^2_{IP} corrections based on finer binning in η and momentum to further improve the agreement, as shown in Fig. 2 for the proton from $\Lambda_b^0 \to \Lambda_c^+\pi^-$ decays in 2018 data and simulation. A similar level of agreement is obtained for the kaon and pions. The same corrections are applied to the $\Xi_b^0 \to \Xi_c^+\pi^-$ decay mode.

The PID response for the final-state hadrons is calibrated using large samples of $D^{*+} \to D^0(K^-\pi^+)\pi^+$ and $\Lambda_b^0 \to \Lambda_c^+\pi^-$ decays [28], where no PID requirements are imposed. Using the calibration data, the PID response for each hadron type is parametrized as a function of its transverse and total momentum, as well as the track multiplicity in the event [29]. The PID response of each hadron in simulated signal decays is updated to use the response obtained from these calibration data, sampled from the relevant PID probability distribution. All PID requirements applied to the simulated signal decays use these calibrated values.

B. Multivariate selection

To suppress background caused by random combinations of reconstructed particles, particularly in the Ξ_b^0 decay mode, a gradient-boosted decision tree (BDT) classifier [30,31] is employed. The training variables of the Λ_b^0 (Ξ_b^0) BDT classifier include the H_b decay vertex-fit χ^2 and $\cos(\theta_{\mathrm{PV}})$, where θ_{PV} is the angle between the H_b momentum vector and the vector that connects the PV and H_b decay vertex; the H_c decay vertex-fit χ^2 and the H_c baryon decay time; and for each final-state particle, the p, p_{T}, χ^2_{IP} values and a PID variable providing a measure of the likelihood that the PID information is consistent with the particle hypothesis [28].

The signal distributions are taken from simulated signal decays with all weights applied. The background sample for the Ξ_b^0 (Λ_b^0) mode is taken from the high-mass sideband region, 5900–6100 MeV/c^2 (5750–5950 MeV/c^2), after all selection criteria are applied. For the Ξ_b^0 decay, the Ξ_c^+ mass requirement is relaxed to include candidates within 30 MeV/c^2 of the known Ξ_c^+ mass [25] to increase the size of the background sample. A loose requirement is applied to the BDT algorithm output, which provides a signal efficiency of about 99%, while suppressing the combinatorial background by a factor of four (three) for the Λ_b^0 (Ξ_b^0) decay mode. After the BDT requirement, less than 1% of events have more than one H_b candidate, and all candidates are retained [32].

C. Fits to the mass distributions

The mass spectra from the full sample for selected candidates are shown in Fig. 3, along with the results of binned extended maximum-likelihood fits [33]. Each mass spectrum is described by the sum of a signal function and three background shapes. The signal-mass shapes are parameterized by the sum of two Crystal Ball

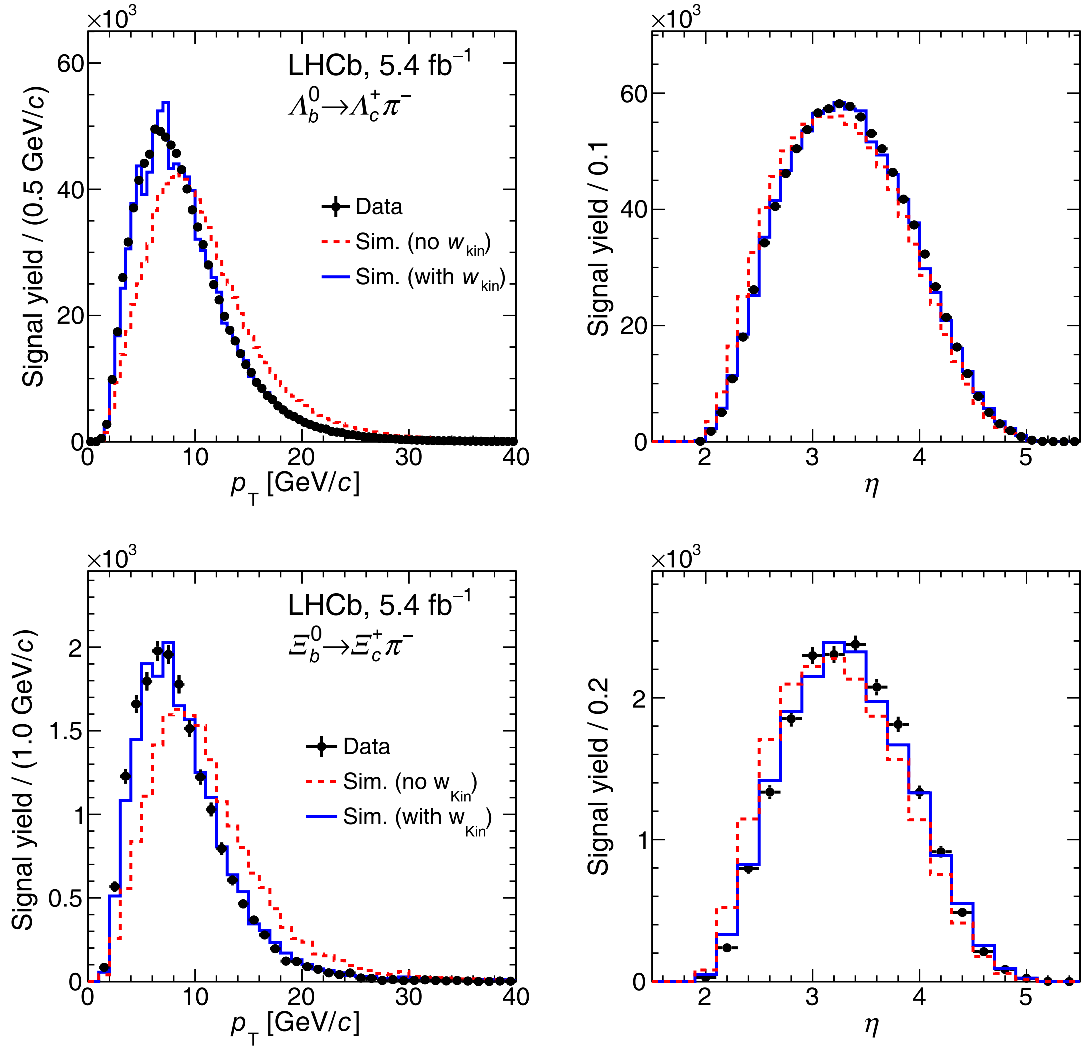

FIG. 1. Comparison of the (left) p_T and (right) η spectra between background-subtracted data and simulation (Sim.), before (red dashed line), and after (blue line) the kinematic and TOS/TIS weights (w_{kin}) are applied. The top row shows the distributions for the Λ_b^0 decay mode and the bottom shows those for the Ξ_b^0 mode.

functions [34] with a common peak position. The signal shape parameters are fixed to the values obtained from simulation, except for the peak position and an overall scale factor, which accounts for a small difference in the mass resolution between data and simulation. In fits to the data, the resulting scale factor is about 1.10, which is close to the value obtained for the measurement of the Ξ_b^- baryon lifetime [7].

The mass shapes of misidentified $H_b \to H_c K^-$ decays are also described using the sum of two Crystal Ball functions [34], with shape parameters fixed to the values obtained from simulated $\Lambda_b^0 \to \Lambda_c^+ K^-$ decays. Taking into account the ratio of branching fractions $\mathcal{B}(\Lambda_b^0 \to \Lambda_c^+ K^-)/\mathcal{B}(\Lambda_b^0 \to \Lambda_c^+ \pi^-)$ [25] and the relative selection efficiency, it is estimated that the yield fraction $N(H_b \to H_c K^-)/N(H_b \to H_c \pi^-)$ is $(3.1 \pm 0.6)\%$ for the Λ_b^0 mode, and $(3.1 \pm 0.9)\%$ for the Ξ_b^0 decay. An additional 20% relative uncertainty is included for the Ξ_b^0 mode to account for an assumption that the relative branching fraction between the Cabibbo-suppressed and Cabibbo-favored mode is equal to that of the Λ_b^0 baryon [25]. These fractions are constrained in the fit with Gaussian priors. Toward the lower edges of the mass distributions there are small contributions from partially reconstructed b -hadron decays with a missing pion or photon(s). The partially reconstructed background is modeled with an Argus shape [35] convolved with a Gaussian resolution function. The shape parameters are obtained from a fit to the data in a wider mass region, and then fixed to those values in the default mass fits. The combinatorial background is described by an exponential function with the shape parameter free to vary in the fit. The Ξ_b^0 and Λ_b^0 signal yields for each L0 category and both L0 categories combined are given in Table I.

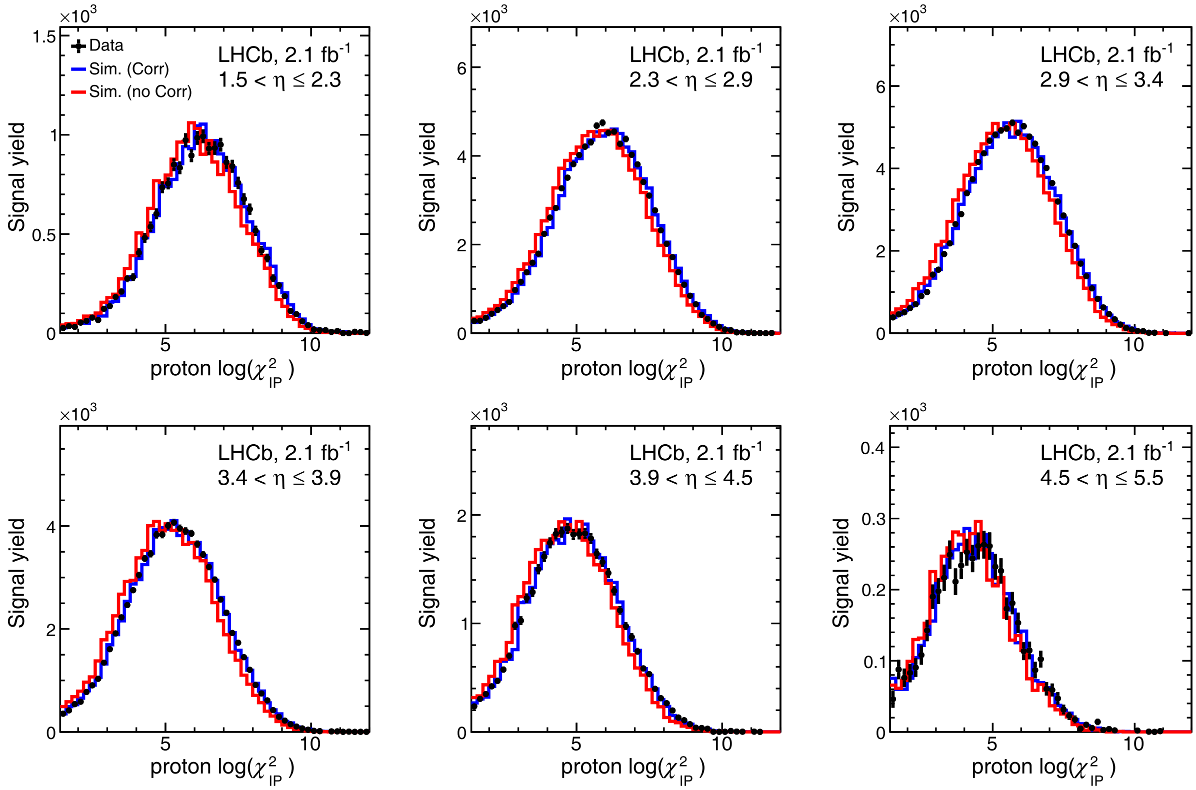

FIG. 2. Distributions of $\log(\chi^2_{\rm IP})$ for background-subtracted 2018 data, uncorrected simulation (red line), and corrected simulation (blue line) for the proton from $\Lambda_b^0 \to \Lambda_c^+\pi^-$ decays. The plots show the distributions in six η regions of the proton.

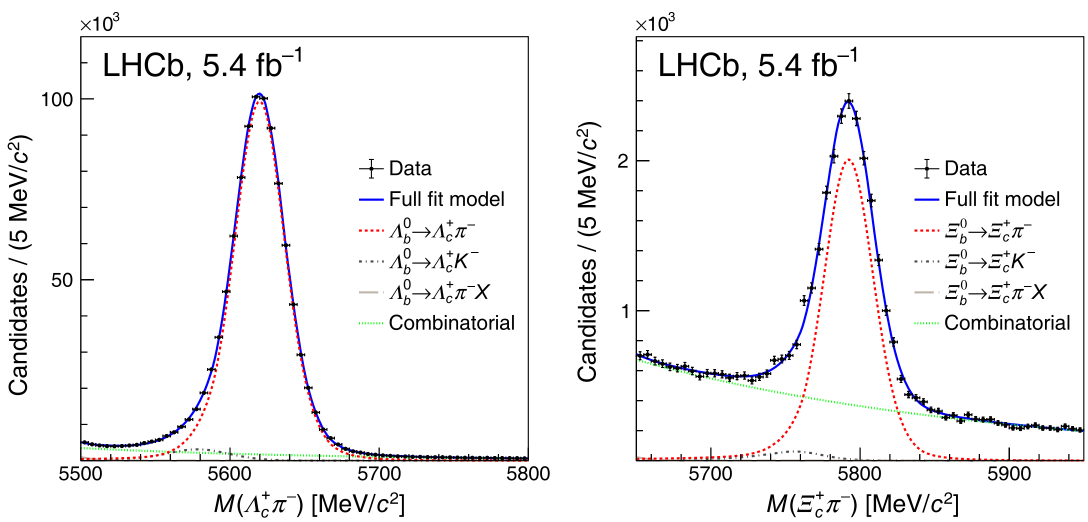

FIG. 3. Mass spectra for (left) $\Lambda_b^0 \to \Lambda_c^+\pi^-$ and (right) $\Xi_b^0 \to \Xi_c^+\pi^-$ candidates in the data. The fit results and projections from the different components, as described in the text, are also shown.

IV. DETERMINATION OF r_τ

The determination of the lifetime ratio r_τ requires the ratio of signal yields and the ratio of selection efficiencies, as shown in Eq. (1). The yields $N[\Xi_b^0 \to \Xi_c^+\pi^-](t)$ and $N[\Lambda_b^0 \to \Lambda_c^+\pi^-](t)$ are determined by fitting the combined TOS + TIS H_b mass spectra in decay-time bins, ranging from 0.4 to 10.0 ps. Specifically, the bin widths are 0.2 ps from $[0.4, 1.8]$ ps, 0.4 ps from $[1.8, 3.0]$ ps, 0.5 ps from $[3.0, 4.0]$ ps, and one bin each from $[4.0, 5.0]$, $[5.0, 7.0]$, and $[7.0, 10.0]$ ps. The mass fits are performed as described previously, where the signal shape parameters in each

TABLE I. Signal yields by hardware trigger category for Λ_b^0 and Ξ_b^0 decays for the total 2016–2018 dataset after all selection requirements. Each yield is obtained from an independent fit to the respective mass spectrum.

b baryon	TOS	TIS	TOS + TIS
Ξ_b^0 ($\times 10^3$)	10.1 ± 0.1	8.1 ± 0.1	18.1 ± 0.2
Λ_b^0 ($\times 10^3$)	520.7 ± 0.9	408.2 ± 0.8	929.1 ± 1.2

decay-time bin are obtained from the corresponding fit to the simulated signal decays in the same decay-time bin, with all weights applied. For the Ξ_b^0 mode, the mass-resolution scale factor is constrained by a Gaussian prior to the value obtained from the fit to the full data sample. The independence of the decay-time resolution on decay time is validated with simulation. All signal and background yields are free parameters in the fit for each decay-time bin. The yields of Λ_b^0 and Ξ_b^0 baryon decays as a function of the decay time are shown in Fig. 4 (left), along with the ratio of yields, $N(\Xi_b^0)/N(\Lambda_b^0)$.

The selection efficiencies for decays within the LHCb acceptance are obtained from simulation, corrected for data-simulation differences as detailed in Sec. III A. The resulting efficiencies versus decay time are shown in Fig. 4 (right). The Λ_b^0 and Ξ_b^0 signal efficiencies show a steep rise from zero decay time, primarily due to the $\chi^2_{\rm IP}$ requirements in the trigger and selection. For the lifetime determination, the H_b decay time is required to be larger than 0.4 ps. As shown in the bottom plots of Fig. 4, the increase in the yield ratio $N(\Xi_b^0)/N(\Lambda_b^0)$ at low decay time trends in the opposite direction to the ratio of selection efficiencies $\varepsilon(\Lambda_b^0)/\varepsilon(\Xi_b^0)$, as one would expect based on the longer Ξ_c^+ baryon lifetime compared to that of the Λ_c^+ baryon.

The product of the yield and efficiency ratios shown in Fig. 4 (bottom) gives $R(t)$, and the result is shown in Fig. 5 (top). The results of a fit to an exponential function are also shown, yielding $\lambda = (2.5 \pm 6.4) \times 10^{-3}\ \text{ps}^{-1}$, with a χ^2 per degree of freedom of 1.04. The uncertainties shown are due to the finite signal yields in the data. From this value, the relative lifetime and Ξ_b^0 lifetime are computed to be

$$r_\tau = 1.004 \pm 0.009,$$

$$\tau_{\Xi_b^0} = 1.473 \pm 0.014\ \text{ps},$$

where the uncertainties are statistical only.

Figure 5 (bottom) compares the Ξ_b^0 baryon decay-time spectrum in background-subtracted data to that of the simulation weighted to represent the measured Ξ_b^0 lifetime. The simulation using the fitted lifetime provides a good description of the spectrum observed in the data.

V. CROSS-CHECKS AND SYSTEMATIC UNCERTAINTIES

A number of cross-checks are performed, where the data are separated into statistically independent subsamples, and the r_τ value is measured in each of these subsamples. The subsamples are partitioned according to (a) data-taking year, (b) TOS and TIS, (c) polarity of the LHCb magnet, (d) number of tracks per event (< 150 or ≥ 150), and (e) number of primary vertices ($n\text{PV} = 1$ or $n\text{PV} \geq 2$). In all cases, the r_τ values are statistically consistent with each other. Among the 11 subsamples, the largest deviation from the overall average is about 1.2σ.

Several sources of systematic uncertainty are considered and shown in Table II, along with their associated values. For each of the sources, unless otherwise indicated, the systematic uncertainty is assessed by making a change to the default method, and assigning the relative change in r_τ with respect to the baseline value as the systematic uncertainty. The total systematic uncertainty is obtained from the quadrature sum of the values from each individual source.

The systematic uncertainty due to the finite simulated sample sizes is obtained by performing 1000 alternative fits for r_τ, where in each fit the relative efficiency in each bin is fluctuated by its uncertainty according to a Gaussian distribution. The standard deviation of the 1000 alternative fits is assigned as the systematic uncertainty.

The sensitivity to the signal shape model is assessed by using an alternative signal model composed of the sum of a Bukin [37] and a Gaussian function with a common peak value. As in the baseline fit, the parameters are determined from simulation and fixed in the mass fits, apart from a scaling of the resolution and the peak mass value. Similarly, the uncertainty due to a specific choice for the combinatorial background model is estimated by redoing the analysis using a third-order (second-order) Chebyshev polynomial for the Λ_b^0 (Ξ_b^0) mass fits instead of an exponential function.

In the baseline fit, background from the unobserved decay $\Xi_b^0 \to \Xi_c^{\prime +}\pi^-$ with $\Xi_c^{\prime +} \to \Xi_c^+\gamma$, has been neglected. In one model calculation [38], the ratio of partial widths is small, $\Gamma(\Xi_b \to \Xi_c^{\prime +}\pi)/\Gamma(\Xi_b \to \Xi_c\pi) \simeq 6.3\%$. The fractional contribution is taken to be $(5.3 \pm 0.6)\%$, which includes a correction for the fraction of decays in the fit range. The shape of this partially reconstructed background is parameterized using RAPIDSIM [39] and included in the mass fits with the fractional contribution constrained by Gaussian prior to the value above. The newly obtained Ξ_b^0 signal yields lead to a modified value of r_τ, and the relative change from the baseline result is assigned as the systematic uncertainty.

For the efficiency determination, the reconstructed signal decays in the simulation are required to be truth-matched with the generated signal decays. In about 7% of cases, this

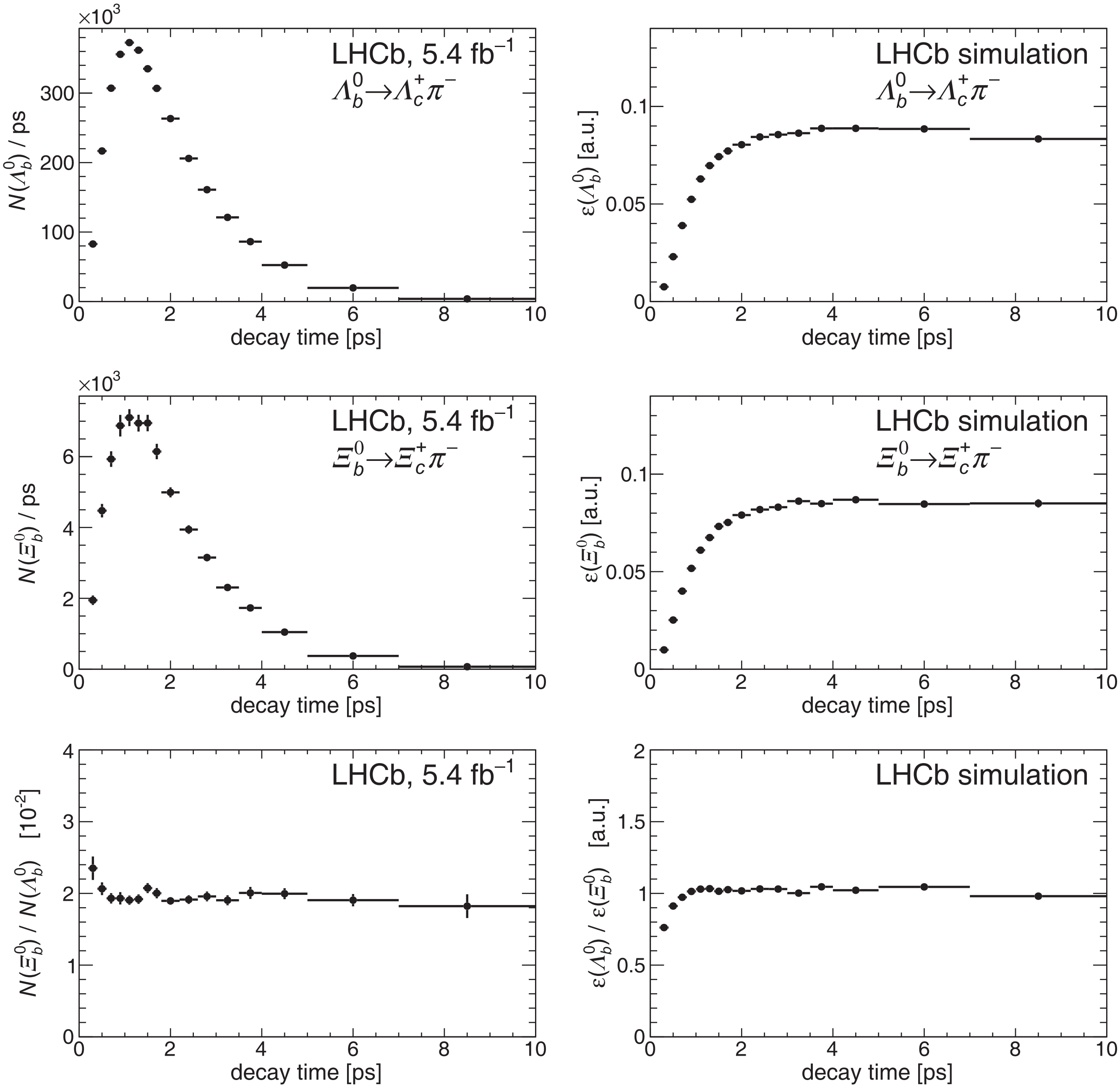

FIG. 4. Left: decay time dependence of the signal yields divided by the bin width for the (top) Λ_b^0 mode, (middle) Ξ_b^0, and (bottom) the ratio $N(\Xi_b^0)/N(\Lambda_b^0)$. Right: decay time dependence of the selection efficiencies for the (top) Λ_b^0 mode, (middle) Ξ_b^0 mode, and (bottom) the ratio $\varepsilon(\Lambda_b^0)/\varepsilon(\Xi_b^0)$, obtained from the weighted simulation. The uncertainties shown are due to the finite number of events in the data and simulation samples.

association fails due to having too few hits on the reconstructed tracks that match to the true hits of each final-state particle. The potential impact of the truth-matching requirement is assessed by removing the matching requirement entirely for the efficiency determination.

The fits are binned extended maximum-likelihood fits, and the baseline bin width is 5.0 MeV$/c^2$ for both the Λ_b^0 and Ξ_b^0 mass fits. In an alternative set of fits, the corresponding bin widths are reduced to 1.0 MeV$/c^2$ and 2.5 MeV$/c^2$, the fits are redone, and the relative difference is assigned as a systematic uncertainty. To study the effects of the binning in decay time, the number of decay-time bins is increased from 17 to 24. The mass fits in the narrower decay-time bins are repeated, leading to a new set of data points for $R(t)$. The relative change from the baseline result is assigned as a systematic uncertainty.

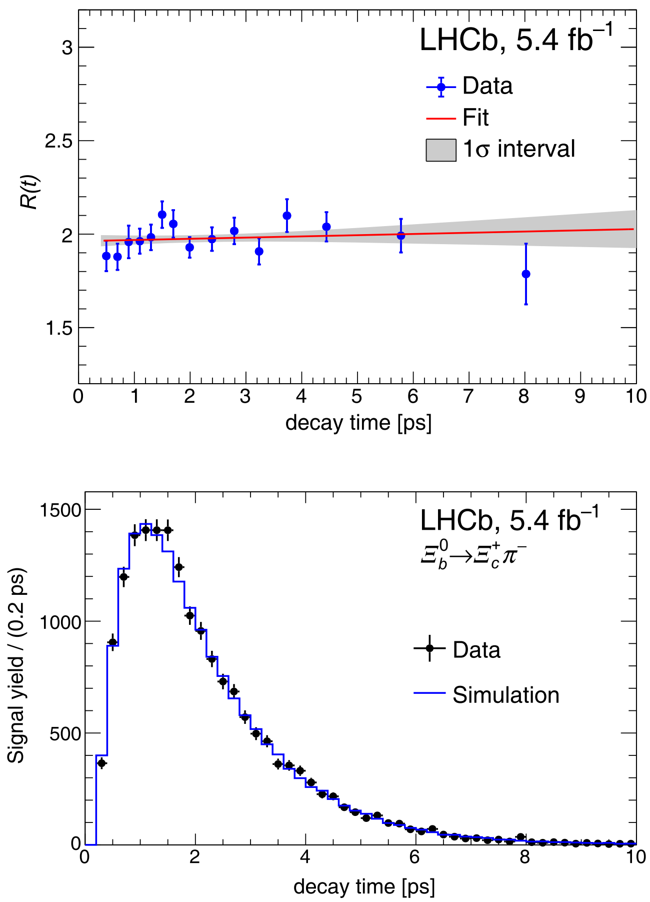

FIG. 5. Top: efficiency-corrected yield ratio $R(t)$ as a function of the decay time. The red line shows the fit result, and the gray band shows the confidence interval at one standard deviation (σ). The points are placed along the time axis at the average within the bin [36], assuming a decay-time spectrum that is exponential with an effective lifetime of 1.47 ps. Bottom: decay-time spectrum of Ξ_b^0 signal decays, along with the simulation using the best-fit lifetime of 1.473 ps.

The BDT performances in data and simulation do not match perfectly for the signal and normalization modes. Since the BDT uses decay-time biasing variables, mainly χ^2_{IP}, differences in the BDT output could be indicative of an imperfect modeling of such input variables and their correlations with other input variables. To assess the potential impact, the ratio of the BDT response in background-subtracted data [27] to simulation is obtained, and used as an additional weight in the determination of the efficiencies $\varepsilon[H_b \to H_c\pi^-](t)$. The resulting fractional change in r_τ is assigned as a systematic uncertainty.

Due to the small value of λ and the precisely known Λ_b^0 baryon lifetime, $\tau_{\Lambda_b^0} = 1.468 \pm 0.009$ ps [25], the systematic uncertainty in r_τ is negligible. The total systematic uncertainty on r_τ is 0.58%, which is subdominant compared to the statistical precision of 0.94%.

TABLE II. Sources and values of the relative systematic uncertainty on the lifetime ratio measurement.

Source	Value (%)
Simulated sample size	0.31
Signal shape	0.28
Background shape	0.02
$\Xi_b^0 \to \Xi_c'^+\pi^-$ background	0.15
Truth matching	0.03
Bin width in mass	0.10
Bin width in time	0.06
BDT requirement	0.36
Λ_b^0 lifetime	0.00
Total	0.58

VI. RESULTS AND SUMMARY

From a pp collision data sample corresponding to an integrated luminosity of 5.4 fb^{-1}, the LHCb collaboration measures the ratio of lifetimes of the Ξ_b^0 baryon relative to that of the Λ_b^0 baryon to be

$$r_\tau^{\mathrm{Run\,2}} = 1.004 \pm 0.009 \pm 0.006,$$

where the uncertainties are statistical and systematic, respectively. Multiplying this ratio by the known Λ_b^0 baryon lifetime, the Ξ_b^0 baryon lifetime is found to be

$$\tau_{\Xi_b^0}^{\mathrm{Run\,2}} = 1.473 \pm 0.014 \pm 0.009 \pm 0.009 \text{ ps},$$

where the last uncertainty is due to that of the Λ_b^0 baryon lifetime.

The value of r_τ is consistent with and about two times more precise than the value $1.006 \pm 0.018 \pm 0.010$ obtained using Run 1 data [8]. The two results are combined taking only the finite sample sizes of the simulated samples as uncorrelated. The rest of the systematic uncertainties are taken to be 100% correlated. Using the BLUE package [40], the Run 1–2 average values are

$$r_\tau = 1.004 \pm 0.008 \pm 0.005,$$
$$\tau_{\Xi_b^0} = 1.475 \pm 0.012 \pm 0.008 \pm 0.009 \text{ ps}.$$

This corresponds to a precision on the lifetime ratio of 1%, which represents an improvement on the Run 1 value by about a factor of two. The measured value is in agreement with the prediction from the heavy-quark expansion, of $r_\tau^{\mathrm{HQE}} = 1.002 \pm 0.023$ [3]. This prediction only accounts for the decay width of the b quark and higher-order corrections. Decays of the Ξ_b^- baryon involving the weak $s \to u\bar{u}d$ transition have been observed by the LHCb collaboration, with branching fraction $\mathcal{B}(\Xi_b^- \to \Lambda_b^0 \pi^-) \sim 1\%$ [41]. Similar decays are expected for the Ξ_b^0 baryon [42,43], which would reduce the central value of the theoretical prediction by about 0.5%. After applying this correction the theoretical calculation would still be in agreement with the measured r_τ value.

ACKNOWLEDGMENTS

We express our gratitude to our colleagues in the CERN accelerator departments for the excellent performance of the LHC. We thank the technical and administrative staff at the LHCb institutes. We acknowledge support from CERN and from the national agencies: ARC (Australia); CAPES, CNPq, FAPERJ and FINEP (Brazil); MOST and NSFC (China); CNRS/IN2P3 (France); BMBF, DFG and MPG (Germany); INFN (Italy); NWO (Netherlands); MNiSW and NCN (Poland); MCID/IFA (Romania); MICIU and AEI (Spain); SNSF and SER (Switzerland); NASU (Ukraine); STFC (United Kingdom); DOE NP and NSF (USA). We acknowledge the computing resources that are provided by ARDC (Australia), CBPF (Brazil), CERN, IHEP and LZU (China), IN2P3 (France), KIT and DESY (Germany), INFN (Italy), SURF (Netherlands), Polish WLCG (Poland), IFIN-HH (Romania), PIC (Spain), CSCS (Switzerland), and GridPP (United Kingdom). We are indebted to the communities behind the multiple open-source software packages on which we depend. Individual groups or members have received support from Key Research Program of Frontier Sciences of CAS, CAS PIFI, CAS CCEPP, Fundamental Research Funds for the Central Universities, and Sci. & Tech. Program of Guangzhou (China); Minciencias (Colombia); EPLANET, Marie Skłodowska-Curie Actions, ERC and NextGenerationEU (European Union); A*MIDEX, ANR, IPhU and Labex P2IO, and Région Auvergne-Rhône-Alpes (France); Alexander-von-Humboldt Foundation (Germany); ICSC (Italy); Severo Ochoa and María de Maeztu Units of Excellence, GVA, XuntaGal, GENCAT, InTalent-Inditex and Prog. Atracción Talento CM (Spain); SRC (Sweden); the Leverhulme Trust, the Royal Society and UKRI (United Kingdom).

DATA AVAILABILITY

The data that support the findings of this article are openly available [44], embargo periods may apply.

[1] A. Lenz, Lifetimes and heavy quark expansion, Int. J. Mod. Phys. A **30**, 1543005 (2015).

[2] N. Cabibbo, Unitary symmetry and leptonic decays, Phys. Rev. Lett. **10**, 531 (1963); M. Kobayashi and T. Maskawa, *CP* -violation in the renormalizable theory of weak interaction, Prog. Theor. Phys. **49**, 652 (1973).

[3] J. Gratrex, A. Lenz, B. Melić, I. Nišandžić, M. L. Piscopo, and A. V. Rusov, Quark-hadron duality at work: Lifetimes of bottom baryons, J. High Energy Phys. 04 (2023) 034.

[4] B. M. Dassinger, T. Mannel, and S. Turczyk, Inclusive semi-leptonic B decays to order $1/m_b^4$, J. High Energy Phys. 03 (2007) 087.

[5] I. Bigi, M. Shifman, N. G. Uraltsev, and A. Vainshtein, Sum rules for heavy flavor transitions in the small velocity limit, Phys. Rev. D **52**, 196 (1995).

[6] T. Mannel, Higher order 1/m corrections at zero recoil, Phys. Rev. D **50**, 428 (1994).

[7] R. Aaij *et al.* (LHCb Collaboration), Precision measurement of the Ξ_b^- baryon lifetime, Phys. Rev. D **110**, 072002 (2024).

[8] R. Aaij *et al.* (LHCb Collaboration), Precision measurement of the mass and lifetime of the Ξ_b^0 baryon, Phys. Rev. Lett. **113**, 032001 (2014).

[9] A. A. Alves Jr. *et al.* (LHCb Collaboration), The LHCb detector at the LHC, J. Instrum. **3**, S08005 (2008).

[10] R. Aaij *et al.* (LHCb Collaboration), LHCb detector performance, Int. J. Mod. Phys. A **30**, 1530022 (2015).

[11] R. Aaij *et al.*, Performance of the LHCb vertex locator, J. Instrum. **9**, P09007 (2014).

[12] P. d'Argent *et al.*, Improved performance of the LHCb outer tracker in LHC run 2, J. Instrum. **12**, P11016 (2017).

[13] M. Adinolfi *et al.*, Performance of the LHCb RICH detector at the LHC, Eur. Phys. J. C **73**, 2431 (2013).

[14] A. A. Alves Jr. *et al.*, Performance of the LHCb muon system, J. Instrum. **8**, P02022 (2013).

[15] R. Aaij *et al.*, Design and performance of the LHCb trigger and full real-time reconstruction in Run 2 of the LHC, J. Instrum. **14**, P04013 (2019).

[16] V. V. Gligorov and M. Williams, Efficient, reliable and fast high-level triggering using a bonsai boosted decision tree, J. Instrum. **8**, P02013 (2013).

[17] T. Likhomanenko, P. Ilten, E. Khairullin, A. Rogozhnikov, A. Ustyuzhanin, and M. Williams, LHCb topological trigger reoptimization, J. Phys. Conf. Ser. **664**, 082025 (2015).

[18] T. Sjöstrand, S. Mrenna, and P. Skands, A brief introduction to PYTHIA 8.1, Comput. Phys. Commun. **178**, 852 (2008); PYTHIA 6.4 physics and manual, J. High Energy Phys. 05 (2006) 026.

[19] I. Belyaev *et al.*, Handling of the generation of primary events in Gauss, the LHCb simulation framework, J. Phys. Conf. Ser. **331**, 032047 (2011).

[20] D. J. Lange, The EvtGen particle decay simulation package, Nucl. Instrum. Methods Phys. Res., Sect. A **462**, 152 (2001).

[21] N. Davidson, T. Przedzinski, and Z. Was, PHOTOS interface in C++: Technical and physics documentation, Comput. Phys. Commun. **199**, 86 (2016).

[22] J. Allison *et al.* (Geant4 Collaboration), Geant4 developments and applications, IEEE Trans. Nucl. Sci. **53**, 270 (2006); S. Agostinelli *et al.* (Geant4 Collaboration), Geant4: A simulation toolkit, Nucl. Instrum. Methods Phys. Res., Sect. A **506**, 250 (2003).

[23] M. Clemencic, G. Corti, S. Easo, C. R. Jones, S. Miglioranzi, M. Pappagallo, and P. Robbe, The LHCb simulation application, Gauss: Design, evolution and experience, J. Phys. Conf. Ser. **331**, 032023 (2011).

[24] D. Müller, M. Clemencic, G. Corti, and M. Gersabeck, ReDecay: A novel approach to speed up the simulation at LHCb, Eur. Phys. J. C **78**, 1009 (2018).

[25] S. Navas *et al.* (Particle Data Group), Review of particle physics, Phys. Rev. D **110**, 030001 (2024).

[26] R. Aaij *et al.*, The LHCb trigger and its performance in 2011, J. Instrum. **8**, P04022 (2013).

[27] M. Pivk and F. R. Le Diberder, sPlot: A statistical tool to unfold data distributions, Nucl. Instrum. Methods Phys. Res., Sect. A **555**, 356 (2005).

[28] R. Aaij *et al.*, Selection and processing of calibration samples to measure the particle identification performance of the LHCb experiment in Run 2, Eur. Phys. J. Tech. Instr. **6**, 1 (2019).

[29] A. Poluektov, Kernel density estimation of a multidimensional efficiency profile, J. Instrum. **10**, P02011 (2015).

[30] Y. Freund and R. E. Schapire, A decision-theoretic generalization of on-line learning and an application to boosting, J. Comput. Syst. Sci. **55**, 119 (1997).

[31] H. Voss, A. Hoecker, J. Stelzer, and F. Tegenfeldt, TMVA—toolkit for multivariate data analysis with ROOT, Proc. Sci. ACAT2007 (**2007**) 040.

[32] P. Koppenburg, Statistical biases in measurements with multiple candidates, arXiv:1703.01128.

[33] R. Barlow, Extended maximum likelihood, Nucl. Instrum. Methods Phys. Res., Sect. A **297**, 496 (1990).

[34] T. Skwarnicki, A study of the radiative cascade transitions between the Upsilon-prime and Upsilon resonances, Ph.D. thesis, Institute of Nuclear Physics, Krakow, 1986 [Report No. DESY-F31-86-02].

[35] H. Albrecht *et al.* (ARGUS Collaboration), Exclusive hadronic decays of B mesons, Z. Phys. C **48**, 543 (1990).

[36] G. D. Lafferty and T. R. Wyatt, Where to stick your data points: The treatment of measurements within wide bins, Nucl. Instrum. Methods Phys. Res., Sect. A **355**, 541 (1995).

[37] W. Verkerke and D. P. Kirkby, The RooFit toolkit for data modeling, eConf **C0303241**, MOLT007 (2003).

[38] H.-W. Ke, G.-Y. Fang, and Y.-L. Shi, Study on the mixing of Ξ_c and Ξ_c' by the transition $\Xi_b \to \Xi_c^{(\prime)}$, Phys. Rev. D **109**, 073006 (2024).

[39] G. A. Cowan, D. C. Craik, and M. D. Needham, RapidSim: An application for the fast simulation of heavy-quark hadron decays, Comput. Phys. Commun. **214**, 239 (2017).

[40] R. Nisius, BLUE: Combining correlated estimates of physics observables within ROOT using the Best Linear Unbiased Estimate method, SoftwareX **11**, 100468 (2020).

[41] R. Aaij *et al.* (LHCb Collaboration), Observation and branching fraction measurement of the decay $\Xi_b^- \to \Lambda_b^0 \pi^-$, Phys. Rev. D **108**, 072002 (2023).

[42] X. Li and M. B. Voloshin, Decays $\Xi_b \to \Lambda_b \pi$ and diquark correlations in hyperons, Phys. Rev. D **90**, 033016 (2014).

[43] M. B. Voloshin, Weak decays $\Xi_Q \to \Lambda_Q \pi$, Phys. Lett. B **476**, 297 (2000).

[44] https://cds.cern.ch/record/2938420

R. Aaij,[38] A. S. W. Abdelmotteleb,[57] C. Abellan Beteta,[51] F. Abudinén,[57] T. Ackernley,[61] A. A. Adefisoye,[69] B. Adeva,[47] M. Adinolfi,[55] P. Adlarson,[85] C. Agapopoulou,[14] C. A. Aidala,[87] Z. Ajaltouni,[11] S. Akar,[11] K. Akiba,[38] P. Albicocco,[28] J. Albrecht,[19,b] R. Aleksiejunas,[80] F. Alessio,[49] P. Alvarez Cartelle,[56] R. Amalric,[16] S. Amato,[3] J. L. Amey,[55] Y. Amhis,[14] L. An,[6] L. Anderlini,[27] M. Andersson,[51] P. Andreola,[51] M. Andreotti,[26] S. Andres Estrada,[84] A. Anelli,[31,49,c] D. Ao,[7] F. Archilli,[37,d] Z Areg,[69] M. Argenton,[26] S. Arguedas Cuendis,[9,49] A. Artamonov,[44] M. Artuso,[69] E. Aslanides,[13] R. Ataíde Da Silva,[50] M. Atzeni,[65] B. Audurier,[12] J. A. Authier,[15] D. Bacher,[64] I. Bachiller Perea,[50] S. Bachmann,[22] M. Bachmayer,[50] J. J. Back,[57] P. Baladron Rodriguez,[47] V. Balagura,[15] A. Balboni,[26] W. Baldini,[26] Z. Baldwin,[78] L. Balzani,[19] H. Bao,[7] J. Baptista de Souza Leite,[61] C. Barbero Pretel,[47,12] M. Barbetti,[27] I. R. Barbosa,[70] R. J. Barlow,[63] M. Barnyakov,[25] S. Barsuk,[14] W. Barter,[59] J. Bartz,[69] S. Bashir,[40] B. Batsukh,[5] P. B. Battista,[14] A. Bay,[50] A. Beck,[65] M. Becker,[19] F. Bedeschi,[35] I. B. Bediaga,[2] N. A. Behling,[19] S. Belin,[47] A. Bellavista,[25] K. Belous,[44] I. Belov,[29] I. Belyaev,[36] G. Benane,[13] G. Bencivenni,[28] E. Ben-Haim,[16] A. Berezhnoy,[44] R. Bernet,[51] S. Bernet Andres,[46] A. Bertolin,[33] C. Betancourt,[51] F. Betti,[59] J. Bex,[56] Ia. Bezshyiko,[51] O. Bezshyyko,[86] J. Bhom,[41] M. S. Bieker,[18] N. V. Biesuz,[26] P. Billoir,[16] A. Biolchini,[38] M. Birch,[62] F. C. R. Bishop,[10] A. Bitadze,[63] A. Bizzeti,[27,e] T. Blake,[57,f] F. Blanc,[50] J. E. Blank,[19] S. Blusk,[69] V. Bocharnikov,[44] J. A. Boelhauve,[19] O. Boente Garcia,[15] T. Boettcher,[68] A. Bohare,[59] A. Boldyrev,[44] C. S. Bolognani,[82] R. Bolzonella,[26,g] R. B. Bonacci,[1] N. Bondar,[44,49] A. Bordelius,[49] F. Borgato,[33,49] S. Borghi,[63] M. Borsato,[31,c] J. T. Borsuk,[83] E. Bottalico,[61] S. A. Bouchiba,[50] M. Bovill,[64] T. J. V. Bowcock,[61] A. Boyer,[49] C. Bozzi,[26] J. D. Brandenburg,[88] A. Brea Rodriguez,[50] N. Breer,[19] J. Brodzicka,[41] A. Brossa Gonzalo,[47,a] J. Brown,[61] D. Brundu,[32]

E. Buchanan,[59] M. Burgos Marcos,[82] A. T. Burke,[63] C. Burr,[49] J. S. Butter,[56] J. Buytaert,[49] W. Byczynski,[49] S. Cadeddu,[32] H. Cai,[75] Y. Cai,[5] A. Caillet,[16] R. Calabrese,[26,g] S. Calderon Ramirez,[9] L. Calefice,[45] S. Cali,[28] M. Calvi,[31,c] M. Calvo Gomez,[46] P. Camargo Magalhaes,[2,h] J. I. Cambon Bouzas,[47] P. Campana,[28] D. H. Campora Perez,[82] A. F. Campoverde Quezada,[7] S. Capelli,[31] M. Caporale,[25] L. Capriotti,[26] R. Caravaca-Mora,[9] A. Carbone,[25,i] L. Carcedo Salgado,[47] R. Cardinale,[29,j] A. Cardini,[32] P. Carniti,[31] L. Carus,[22] A. Casais Vidal,[65] R. Caspary,[22] G. Casse,[61] M. Cattaneo,[49] G. Cavallero,[26] V. Cavallini,[26,g] S. Celani,[22] I. Celestino,[35,k] S. Cesare,[30,l] F. Cesario Laterza Lopes,[2] A. J. Chadwick,[61] I. Chahrour,[87] H. Chang,[4,m] M. Charles,[16] Ph. Charpentier,[49] E. Chatzianagnostou,[38] R. Cheaib,[79] M. Chefdeville,[10] C. Chen,[56] J. Chen,[50] S. Chen,[5] Z. Chen,[7] M. Cherif,[12] A. Chernov,[41] S. Chernyshenko,[53] X. Chiotopoulos,[82] V. Chobanova,[84] M. Chrzaszcz,[41] A. Chubykin,[44] V. Chulikov,[28,36,49] P. Ciambrone,[28] X. Cid Vidal,[47] G. Ciezarek,[49] P. Cifra,[38] P. E. L. Clarke,[59] M. Clemencic,[49] H. V. Cliff,[56] J. Closier,[49] C. Cocha Toapaxi,[22] V. Coco,[49] J. Cogan,[13] E. Cogneras,[11] L. Cojocariu,[43] S. Collaviti,[50] P. Collins,[49] T. Colombo,[49] M. Colonna,[19] A. Comerma-Montells,[45] L. Congedo,[24] J. Connaughton,[57] A. Contu,[32] N. Cooke,[60] G. Cordova,[35,k] C. Coronel,[66] I. Corredoira,[12] A. Correia,[16] G. Corti,[49] J. Cottee Meldrum,[55] B. Couturier,[49] D. C. Craik,[51] M. Cruz Torres,[2,n] E. Curras Rivera,[50] R. Currie,[59] C. L. Da Silva,[68] S. Dadabaev,[44] L. Dai,[72] X. Dai,[4] E. Dall'Occo,[49] J. Dalseno,[84] C. D'Ambrosio,[62] J. Daniel,[11] P. d'Argent,[24] G. Darze,[3] A. Davidson,[57] J. E. Davies,[63] O. De Aguiar Francisco,[63] C. De Angelis,[32,o] F. De Benedetti,[49] J. de Boer,[38] K. De Bruyn,[81] S. De Capua,[63] M. De Cian,[63] U. De Freitas Carneiro Da Graca,[2,p] E. De Lucia,[28] J. M. De Miranda,[2] L. De Paula,[3] M. De Serio,[24,q] P. De Simone,[28] F. De Vellis,[19] J. A. de Vries,[82] F. Debernardis,[24] D. Decamp,[10] S. Dekkers,[1] L. Del Buono,[16] B. Delaney,[65] H.-P. Dembinski,[19] J. Deng,[8] V. Denysenko,[51] O. Deschamps,[11] F. Dettori,[32,o] B. Dey,[79] P. Di Nezza,[28] I. Diachkov,[44] S. Didenko,[44] S. Ding,[69] Y. Ding,[50] L. Dittmann,[22] V. Dobishuk,[53] A. D. Docheva,[60] A. Doheny,[57] C. Dong,[4,m] A. M. Donohoe,[23] F. Dordei,[32] A. C. dos Reis,[2] A. D. Dowling,[69] L. Dreyfus,[13] W. Duan,[73] P. Duda,[83] L. Dufour,[49] V. Duk,[34] P. Durante,[49] M. M. Duras,[83] J. M. Durham,[68] O. D. Durmus,[79] A. Dziurda,[41] A. Dzyuba,[44] S. Easo,[58] E. Eckstein,[18] U. Egede,[1] A. Egorychev,[44] V. Egorychev,[44] S. Eisenhardt,[59] E. Ejopu,[63] L. Eklund,[85] M. Elashri,[66] J. Ellbracht,[19] S. Ely,[62] A. Ene,[43] J. Eschle,[69] S. Esen,[22] T. Evans,[38] F. Fabiano,[32] S. Faghih,[66] L. N. Falcao,[2] B. Fang,[7] R. Fantechi,[35] L. Fantini,[34,r] M. Faria,[50] K. Farmer,[59] D. Fazzini,[31,c] L. Felkowski,[83] M. Feng,[5,7] M. Feo,[19] A. Fernandez Casani,[48] M. Fernandez Gomez,[47] A. D. Fernez,[67] F. Ferrari,[25,i] F. Ferreira Rodrigues,[3] M. Ferrillo,[51] M. Ferro-Luzzi,[49] S. Filippov,[44] R. A. Fini,[24] M. Fiorini,[26,g] M. Firlej,[40] K. L. Fischer,[64] D. S. Fitzgerald,[87] C. Fitzpatrick,[63] T. Fiutowski,[40] F. Fleuret,[15] A. Fomin,[52] M. Fontana,[25] L. F. Foreman,[63] R. Forty,[49] D. Foulds-Holt,[59] V. Franco Lima,[3] M. Franco Sevilla,[67] M. Frank,[49] E. Franzoso,[26,g] G. Frau,[63] C. Frei,[49] D. A. Friday,[63,49] J. Fu,[7] Q. Führing,[19,56,b] T. Fulghesu,[13] G. Galati,[24] M. D. Galati,[38] A. Gallas Torreira,[47] D. Galli,[25,i] S. Gambetta,[59] M. Gandelman,[3] P. Gandini,[30] B. Ganie,[63] H. Gao,[7] R. Gao,[64] T. Q. Gao,[56] Y. Gao,[8] Y. Gao,[6] Y. Gao,[8] L. M. Garcia Martin,[50] P. Garcia Moreno,[45] J. García Pardiñas,[65] P. Gardner,[67] K. G. Garg,[8] L. Garrido,[45] C. Gaspar,[49] A. Gavrikov,[33] L. L. Gerken,[19] E. Gersabeck,[20] M. Gersabeck,[20] T. Gershon,[57] S. Ghizzo,[29,j] Z. Ghorbanimoghaddam,[55] L. Giambastiani,[33,s] F. I. Giasemis,[16,t] V. Gibson,[56] H. K. Giemza,[42] A. L. Gilman,[64] M. Giovannetti,[28] A. Gioventù,[45] L. Girardey,[63,58] M. A. Giza,[41] F. C. Glaser,[14,22] V. V. Gligorov,[16] C. Göbel,[70] L. Golinka-Bezshyyko,[86] E. Golobardes,[46] D. Golubkov,[44] A. Golutvin,[62,49] S. Gomez Fernandez,[45] W. Gomulka,[40] I. Gonçales Vaz,[49] F. Goncalves Abrantes,[64] M. Goncerz,[41] G. Gong,[4,m] J. A. Gooding,[19] I. V. Gorelov,[44] C. Gotti,[31] E. Govorkova,[65] J. P. Grabowski,[18] L. A. Granado Cardoso,[49] E. Graugés,[45] E. Graverini,[50,u] L. Grazette,[57] G. Graziani,[27] A. T. Grecu,[43] L. M. Greeven,[38] N. A. Grieser,[66] L. Grillo,[60] S. Gromov,[44] C. Gu,[15] M. Guarise,[26] L. Guerry,[11] V. Guliaeva,[44] P. A. Günther,[22] A.-K. Guseinov,[50] E. Gushchin,[44] Y. Guz,[6,49] T. Gys,[49] K. Habermann,[18] T. Hadavizadeh,[1] C. Hadjivasiliou,[67] G. Haefeli,[50] C. Haen,[49] S. Haken,[56] G. Hallett,[57] P. M. Hamilton,[67] J. Hammerich,[61] Q. Han,[33] X. Han,[22,49] S. Hansmann-Menzemer,[22] L. Hao,[7] N. Harnew,[64] T. H. Harris,[1] M. Hartmann,[14] S. Hashmi,[40] J. He,[7,v] A. Hedes,[63] F. Hemmer,[49] C. Henderson,[66] R. Henderson,[14] R. D. L. Henderson,[1] A. M. Hennequin,[49] K. Hennessy,[61] L. Henry,[50] J. Herd,[62] P. Herrero Gascon,[22] J. Heuel,[17] A. Hicheur,[3] G. Hijano Mendizabal,[51] J. Horswill,[63] R. Hou,[8] Y. Hou,[11] D. C. Houston,[60] N. Howarth,[61] J. Hu,[73] W. Hu,[7] X. Hu,[4,m] W. Hulsbergen,[38] R. J. Hunter,[57] M. Hushchyn,[44] D. Hutchcroft,[61] M. Idzik,[40] D. Ilin,[44] P. Ilten,[66]

A. Iniukhin,[44] A. Iohner,[10] A. Ishteev,[44] K. Ivshin,[44] H. Jage,[17] S. J. Jaimes Elles,[77,48,49] S. Jakobsen,[49] E. Jans,[38] B. K. Jashal,[48] A. Jawahery,[67] C. Jayaweera,[54] V. Jevtic,[19] Z. Jia,[16] E. Jiang,[67] X. Jiang,[5,7] Y. Jiang,[7] Y. J. Jiang,[6] E. Jimenez Moya,[9] N. Jindal,[88] M. John,[64] A. John Rubesh Rajan,[23] D. Johnson,[54] C. R. Jones,[56] S. Joshi,[42] B. Jost,[49] J. Juan Castella,[56] N. Jurik,[49] I. Juszczak,[41] D. Kaminaris,[50] S. Kandybei,[52] M. Kane,[59] Y. Kang,[4,m] C. Kar,[11] M. Karacson,[49] A. Kauniskangas,[50] J. W. Kautz,[66] M. K. Kazanecki,[41] F. Keizer,[49] M. Kenzie,[56] T. Ketel,[38] B. Khanji,[69] A. Kharisova,[44] S. Kholodenko,[62,49] G. Khreich,[14] T. Kirn,[17] V. S. Kirsebom,[31,c] O. Kitouni,[65] S. Klaver,[39] N. Kleijne,[35,k] D. K. Klekots,[86] K. Klimaszewski,[42] M. R. Kmiec,[42] S. Koliiev,[53] L. Kolk,[19] A. Konoplyannikov,[6] P. Kopciewicz,[49] P. Koppenburg,[38] A. Korchin,[52] M. Korolev,[44] I. Kostiuk,[38] O. Kot,[53] S. Kotriakhova, E. Kowalczyk,[67] A. Kozachuk,[44] P. Kravchenko,[44] L. Kravchuk,[44] O. Kravcov,[80] M. Kreps,[57] P. Krokovny,[44] W. Krupa,[69] W. Krzemien,[42] O. Kshyvanskyi,[53] S. Kubis,[83] M. Kucharczyk,[41] V. Kudryavtsev,[44] E. Kulikova,[44] A. Kupsc,[85] V. Kushnir,[52] B. Kutsenko,[13] J. Kvapil,[68] I. Kyryllin,[52] D. Lacarrere,[49] P. Laguarta Gonzalez,[45] A. Lai,[32] A. Lampis,[32] D. Lancierini,[62] C. Landesa Gomez,[47] J. J. Lane,[1] G. Lanfranchi,[28] C. Langenbruch,[22] J. Langer,[19] O. Lantwin,[44] T. Latham,[57] F. Lazzari,[35,49,u] C. Lazzeroni,[54] R. Le Gac,[13] H. Lee,[61] R. Lefèvre,[11] A. Leflat,[44] S. Legotin,[44] M. Lehuraux,[57] E. Lemos Cid,[49] O. Leroy,[13] T. Lesiak,[41] E. D. Lesser,[49] B. Leverington,[22] A. Li,[4,m] C. Li,[4] C. Li,[13] H. Li,[73] J. Li,[8] K. Li,[76] L. Li,[63] M. Li,[8] P. Li,[7] P.-R. Li,[74] Q. Li,[5,7] T. Li,[72] T. Li,[73] Y. Li,[8] Y. Li,[5] Y. Li,[4] Z. Lian,[4,m] Q. Liang,[8] X. Liang,[69] Z. Liang,[32] S. Libralon,[48] A. L. Lightbody,[12] C. Lin,[7] T. Lin,[58] R. Lindner,[49] H. Linton,[62] R. Litvinov,[32] D. Liu,[8] F. L. Liu,[1] G. Liu,[73] K. Liu,[74] S. Liu,[5,7] W. Liu,[8] Y. Liu,[59] Y. Liu,[74] Y. L. Liu,[62] G. Loachamin Ordonez,[70] A. Lobo Salvia,[45] A. Loi,[32] T. Long,[56] J. H. Lopes,[3] A. Lopez Huertas,[45] C. Lopez Iribarnegaray,[47] S. López Soliño,[47] Q. Lu,[15] C. Lucarelli,[49] D. Lucchesi,[33,s] M. Lucio Martinez,[48] Y. Luo,[6] A. Lupato,[33,w] E. Luppi,[26,g] K. Lynch,[23] X.-R. Lyu,[7] G. M. Ma,[4,m] S. Maccolini,[19] F. Machefert,[14] F. Maciuc,[43] B. Mack,[69] I. Mackay,[64] L. M. Mackey,[69] L. R. Madhan Mohan,[56] M. J. Madurai,[54] D. Magdalinski,[38] D. Maisuzenko,[44] J. J. Malczewski,[41] S. Malde,[64] L. Malentacca,[49] A. Malinin,[44] T. Maltsev,[44] G. Manca,[32,o] G. Mancinelli,[13] C. Mancuso,[14] R. Manera Escalero,[45] F. M. Manganella,[37] D. Manuzzi,[25] D. Marangotto,[30,l] J. F. Marchand,[10] R. Marchevski,[50] U. Marconi,[25] E. Mariani,[16] S. Mariani,[49] C. Marin Benito,[45] J. Marks,[22] A. M. Marshall,[55] L. Martel,[64] G. Martelli,[34] G. Martellotti,[36] L. Martinazzoli,[49] M. Martinelli,[31,c] D. Martinez Gomez,[81] D. Martinez Santos,[84] F. Martinez Vidal,[48] A. Martorell i Granollers,[46] A. Massafferri,[2] R. Matev,[49] A. Mathad,[49] V. Matiunin,[44] C. Matteuzzi,[69] K. R. Mattioli,[15] A. Mauri,[62] E. Maurice,[15] J. Mauricio,[45] P. Mayencourt,[50] J. Mazorra de Cos,[48] M. Mazurek,[42] M. McCann,[62] T. H. McGrath,[63] N. T. McHugh,[60] A. McNab,[63] R. McNulty,[23] B. Meadows,[66] G. Meier,[19] D. Melnychuk,[42] D. Mendoza Granada,[16] P. Menendez Valdes Perez,[47] F. M. Meng,[4,m] M. Merk,[38,82] A. Merli,[50,30] L. Meyer Garcia,[67] D. Miao,[5,7] H. Miao,[7] M. Mikhasenko,[78] D. A. Milanes,[77,x] A. Minotti,[31,c] E. Minucci,[28] T. Miralles,[11] B. Mitreska,[19] D. S. Mitzel,[19] A. Modak,[58] L. Moeser,[19] R. D. Moise,[17] E. F. Molina Cardenas,[87] T. Mombächer,[49] M. Monk,[57,1] S. Monteil,[11] A. Morcillo Gomez,[47] G. Morello,[28] M. J. Morello,[35,k] M. P. Morgenthaler,[22] J. Moron,[40] W. Morren,[38] A. B. Morris,[49] A. G. Morris,[13] R. Mountain,[69] H. Mu,[4,m] Z. M. Mu,[6] E. Muhammad,[57] F. Muheim,[59] M. Mulder,[81] K. Müller,[51] F. Muñoz-Rojas,[9] R. Murta,[62] V. Mytrochenko,[52] P. Naik,[61] T. Nakada,[50] R. Nandakumar,[58] T. Nanut,[49] I. Nasteva,[3] M. Needham,[59] E. Nekrasova,[44] N. Neri,[30,l] S. Neubert,[18] N. Neufeld,[49] P. Neustroev,[44] J. Nicolini,[49] D. Nicotra,[82] E. M. Niel,[15] N. Nikitin,[44] L. Nisi,[19] Q. Niu,[74] P. Nogarolli,[3] P. Nogga,[18] C. Normand,[55] J. Novoa Fernandez,[47] G. Nowak,[66] C. Nunez,[87] H. N. Nur,[60] A. Oblakowska-Mucha,[40] V. Obraztsov,[44] T. Oeser,[17] A. Okhotnikov,[44] O. Okhrimenko,[53] R. Oldeman,[32,o] F. Oliva,[59,49] E. Olivart Pino,[45] M. Olocco,[19] C. J. G. Onderwater,[82] R. H. O'Neil,[49] J. S. Ordonez Soto,[11] D. Osthues,[19] J. M. Otalora Goicochea,[3] P. Owen,[51] A. Oyanguren,[48] O. Ozcelik,[49] F. Paciolla,[35,y] A. Padee,[42] K. O. Padeken,[18] B. Pagare,[47] T. Pajero,[49] A. Palano,[24] M. Palutan,[28] C. Pan,[75] X. Pan,[4,m] S. Panebianco,[12] G. Panshin,[5] L. Paolucci,[63] A. Papanestis,[58] M. Pappagallo,[24,q] L. L. Pappalardo,[26] C. Pappenheimer,[66] C. Parkes,[63] D. Parmar,[78] B. Passalacqua,[26,g] G. Passaleva,[27] D. Passaro,[35,49,k] A. Pastore,[24] M. Patel,[62] J. Patoc,[64] C. Patrignani,[25,i] A. Paul,[69] C. J. Pawley,[82] A. Pellegrino,[38] J. Peng,[5,7] X. Peng,[74] M. Pepe Altarelli,[28] S. Perazzini,[25] D. Pereima,[44] H. Pereira Da Costa,[68] M. Pereira Martinez,[47] A. Pereiro Castro,[47] C. Perez,[46] P. Perret,[11] A. Perrevoort,[81] A. Perro,[49,13] M. J. Peters,[66] K. Petridis,[55] A. Petrolini,[29,j] S. Pezzulo,[29,j]

J. P. Pfaller,[66] H. Pham,[69] L. Pica,[35,k] M. Piccini,[34] L. Piccolo,[32] B. Pietrzyk,[10] G. Pietrzyk,[14] R. N. Pilato,[61] D. Pinci,[36] F. Pisani,[49] M. Pizzichemi,[31,49,c] V. M. Placinta,[43] M. Plo Casasus,[47] T. Poeschl,[49] F. Polci,[16] M. Poli Lener,[28] A. Poluektov,[13] N. Polukhina,[44] I. Polyakov,[63] E. Polycarpo,[3] S. Ponce,[49] D. Popov,[7,49] S. Poslavskii,[44] K. Prasanth,[59] C. Prouve,[84] D. Provenzano,[32,49,o] V. Pugatch,[53] G. Punzi,[35,u] J. R. Pybus,[68] S. Qasim,[51] Q. Q. Qian,[6] W. Qian,[7] N. Qin,[4,m] S. Qu,[4,m] R. Quagliani,[49] R. I. Rabadan Trejo,[57] R. Racz,[80] J. H. Rademacker,[55] M. Rama,[35] M. Ramírez García,[87] V. Ramos De Oliveira,[70] M. Ramos Pernas,[57] M. S. Rangel,[3] F. Ratnikov,[44] G. Raven,[39] M. Rebollo De Miguel,[48] F. Redi,[30,w] J. Reich,[55] F. Reiss,[20] Z. Ren,[7] P. K. Resmi,[64] M. Ribalda Galvez,[45] R. Ribatti,[50] G. Ricart,[15,12] D. Riccardi,[35,k] S. Ricciardi,[58] K. Richardson,[65] M. Richardson-Slipper,[56] K. Rinnert,[61] P. Robbe,[14,49] G. Robertson,[60] E. Rodrigues,[61] A. Rodriguez Alvarez,[45] E. Rodriguez Fernandez,[47] J. A. Rodriguez Lopez,[77] E. Rodriguez Rodriguez,[49] J. Roensch,[19] A. Rogachev,[44] A. Rogovskiy,[58] D. L. Rolf,[19] P. Roloff,[49] V. Romanovskiy,[66] A. Romero Vidal,[47] G. Romolini,[26,49] F. Ronchetti,[50] T. Rong,[6] M. Rotondo,[28] S. R. Roy,[22] M. S. Rudolph,[69] M. Ruiz Diaz,[22] R. A. Ruiz Fernandez,[47] J. Ruiz Vidal,[82] J. J. Saavedra-Arias,[9] J. J. Saborido Silva,[47] S. E. R. Sacha Emile R.,[49] R. Sadek,[15] N. Sagidova,[44] D. Sahoo,[79] N. Sahoo,[54] B. Saitta,[32,o] M. Salomoni,[31,49,c] I. Sanderswood,[48] R. Santacesaria,[36] C. Santamarina Rios,[47] M. Santimaria,[28] L. Santoro,[2] E. Santovetti,[37] A. Saputi, D. Saranin,[44] A. Sarnatskiy,[81] G. Sarpis,[49] M. Sarpis,[80] C. Satriano,[36,z] A. Satta,[37] M. Saur,[74] D. Savrina,[44] H. Sazak,[17] F. Sborzacchi,[49,28] A. Scarabotto,[19] S. Schael,[17] S. Scherl,[61] M. Schiller,[22] H. Schindler,[49] M. Schmelling,[21] B. Schmidt,[49] N. Schmidt,[68] S. Schmitt,[17] H. Schmitz,[18] O. Schneider,[50] A. Schopper,[62] N. Schulte,[19] M. H. Schune,[14] G. Schwering,[17] B. Sciascia,[28] A. Sciuccati,[49] I. Segal,[78] S. Sellam,[47] A. Semennikov,[44] T. Senger,[51] M. Senghi Soares,[39] A. Sergi,[29,49,j] N. Serra,[51] L. Sestini,[27] A. Seuthe,[19] B. Sevilla Sanjuan,[46] Y. Shang,[6] D. M. Shangase,[87] M. Shapkin,[44] R. S. Sharma,[69] I. Shchemerov,[44] L. Shchutska,[50] T. Shears,[61] L. Shekhtman,[44] Z. Shen,[38] S. Sheng,[5,7] V. Shevchenko,[44] B. Shi,[7] Q. Shi,[7] W. S. Shi,[73] Y. Shimizu,[14] E. Shmanin,[25] R. Shorkin,[44] J. D. Shupperd,[69] R. Silva Coutinho,[69] G. Simi,[33,s] S. Simone,[24,q] M. Singha,[79] N. Skidmore,[57] T. Skwarnicki,[69] M. W. Slater,[54] E. Smith,[65] K. Smith,[68] M. Smith,[62] L. Soares Lavra,[59] M. D. Sokoloff,[66] F. J. P. Soler,[60] A. Solomin,[55] A. Solovev,[44] N. S. Sommerfeld,[18] R. Song,[1] Y. Song,[50] Y. Song,[4,m] Y. S. Song,[6] F. L. Souza De Almeida,[69] B. Souza De Paula,[3] K. M. Sowa,[40] E. Spadaro Norella,[29,j] E. Spedicato,[25] J. G. Speer,[19] P. Spradlin,[60] V. Sriskaran,[49] F. Stagni,[49] M. Stahl,[78] S. Stahl,[49] S. Stanislaus,[64] M. Stefaniak,[88] E. N. Stein,[49] O. Steinkamp,[51] H. Stevens,[19] D. Strekalina,[44] Y. Su,[7] F. Suljik,[64] J. Sun,[32] J. Sun,[63] L. Sun,[75] D. Sundfeld,[2] W. Sutcliffe,[51] V. Svintozelskyi,[48] K. Swientek,[40] F. Swystun,[56] A. Szabelski,[42] T. Szumlak,[40] Y. Tan,[4,m] Y. Tang,[75] Y. T. Tang,[7] M. D. Tat,[22] J. A. Teijeiro Jimenez,[47] A. Terentev,[44] F. Terzuoli,[35,y] F. Teubert,[49] E. Thomas,[49] D. J. D. Thompson,[54] A. R. Thomson-Strong,[59] H. Tilquin,[62] V. Tisserand,[11] S. T'Jampens,[10] M. Tobin,[5,49] T. T. Todorov,[20] L. Tomassetti,[26,g] G. Tonani,[30] X. Tong,[6] T. Tork,[30] D. Torres Machado,[2] L. Toscano,[19] D. Y. Tou,[4,m] C. Trippl,[46] G. Tuci,[22] N. Tuning,[38] L. H. Uecker,[22] A. Ukleja,[40] D. J. Unverzagt,[22] A. Upadhyay,[49] B. Urbach,[59] A. Usachov,[39] A. Ustyuzhanin,[44] U. Uwer,[22] V. Vagnoni,[25] V. Valcarce Cadenas,[47] G. Valenti,[25] N. Valls Canudas,[49] J. van Eldik,[49] H. Van Hecke,[68] E. van Herwijnen,[62] C. B. Van Hulse,[47,aa] R. Van Laak,[50] M. van Veghel,[38] G. Vasquez,[51] R. Vazquez Gomez,[45] P. Vazquez Regueiro,[47] C. Vázquez Sierra,[84] S. Vecchi,[26] J. Velilla Serna,[48] J. J. Velthuis,[55] M. Veltri,[27,bb] A. Venkateswaran,[50] M. Verdoglia,[32] M. Vesterinen,[57] W. Vetens,[69] D. Vico Benet,[64] P. Vidrier Villalba,[45] M. Vieites Diaz,[47,49] X. Vilasis-Cardona,[46] E. Vilella Figueras,[61] A. Villa,[25] P. Vincent,[16] B. Vivacqua,[3] F. C. Volle,[54] D. vom Bruch,[13] N. Voropaev,[44] K. Vos,[82] C. Vrahas,[59] J. Wagner,[19] J. Walsh,[35] E. J. Walton,[1,57] G. Wan,[6] A. Wang,[7] B. Wang,[5] C. Wang,[22] G. Wang,[8] H. Wang,[74] J. Wang,[6] J. Wang,[5] J. Wang,[4,m] J. Wang,[75] M. Wang,[49] N. W. Wang,[7] R. Wang,[55] X. Wang,[8] X. Wang,[73] X. W. Wang,[62] Y. Wang,[76] Y. Wang,[6] Y. H. Wang,[74] Z. Wang,[14] Z. Wang,[4,m] Z. Wang,[30] J. A. Ward,[57] M. Waterlaat,[49] N. K. Watson,[54] D. Websdale,[62] Y. Wei,[6] J. Wendel,[84] B. D. C. Westhenry,[55] C. White,[56] M. Whitehead,[60] E. Whiter,[54] A. R. Wiederhold,[63] D. Wiedner,[19] M. A. Wiegertjes,[38] C. Wild,[64] G. Wilkinson,[64,49] M. K. Wilkinson,[66] M. Williams,[65] M. J. Williams,[49] M. R. J. Williams,[59] R. Williams,[56] S. Williams,[55] Z. Williams,[55] F. F. Wilson,[58] M. Winn,[12] W. Wislicki,[42] M. Witek,[41] L. Witola,[19] T. Wolf,[22] E. Wood,[56] G. Wormser,[14] S. A. Wotton,[56] H. Wu,[69] J. Wu,[8] X. Wu,[75] Y. Wu,[6,56] Z. Wu,[7] K. Wyllie,[49] S. Xian,[73] Z. Xiang,[5] Y. Xie,[8]

T. X. Xing,[30] A. Xu,[35,k] L. Xu,[4,m] L. Xu,[4,m] M. Xu,[49] Z. Xu,[49] Z. Xu,[7] Z. Xu,[5] K. Yang,[62] X. Yang,[6] Y. Yang,[15] Z. Yang,[6] V. Yeroshenko,[14] H. Yeung,[63] H. Yin,[8] X. Yin,[7] C. Y. Yu,[6] J. Yu,[72] X. Yuan,[5] Y Yuan,[5,7] E. Zaffaroni,[50] J. A. Zamora Saa,[71] M. Zavertyaev,[21] M. Zdybal,[41] F. Zenesini,[25] C. Zeng,[5,7] M. Zeng,[4,m] C. Zhang,[6] D. Zhang,[8] J. Zhang,[7] L. Zhang,[4,m] R. Zhang,[8] S. Zhang,[72] S. Zhang,[64] Y. Zhang,[6] Y. Z. Zhang,[4,m] Z. Zhang,[4,m] Y. Zhao,[22] A. Zhelezov,[22] S. Z. Zheng,[6] X. Z. Zheng,[4,m] Y. Zheng,[7] T. Zhou,[6] X. Zhou,[8] Y. Zhou,[7] V. Zhovkovska,[57] L. Z. Zhu,[7] X. Zhu,[4,m] X. Zhu,[8] Y. Zhu,[17] V. Zhukov,[17] J. Zhuo,[48] Q. Zou,[5,7] D. Zuliani,[33,s] and G. Zunica[50]

(LHCb Collaboration)

[1]*School of Physics and Astronomy, Monash University, Melbourne, Australia*
[2]*Centro Brasileiro de Pesquisas Físicas (CBPF), Rio de Janeiro, Brazil*
[3]*Universidade Federal do Rio de Janeiro (UFRJ), Rio de Janeiro, Brazil*
[4]*Department of Engineering Physics, Tsinghua University, Beijing, China*
[5]*Institute Of High Energy Physics (IHEP), Beijing, China*
[6]*School of Physics State Key Laboratory of Nuclear Physics and Technology, Peking University, Beijing, China*
[7]*University of Chinese Academy of Sciences, Beijing, China*
[8]*Institute of Particle Physics, Central China Normal University, Wuhan, Hubei, China*
[9]*Consejo Nacional de Rectores (CONARE), San Jose, Costa Rica*
[10]*Université Savoie Mont Blanc, CNRS, IN2P3-LAPP, Annecy, France*
[11]*Université Clermont Auvergne, CNRS/IN2P3, LPC, Clermont-Ferrand, France*
[12]*Université Paris-Saclay, Centre d'Etudes de Saclay (CEA), IRFU, Saclay, France, Gif-Sur-Yvette, France*
[13]*Aix Marseille Univ, CNRS/IN2P3, CPPM, Marseille, France*
[14]*Université Paris-Saclay, CNRS/IN2P3, IJCLab, Orsay, France*
[15]*Laboratoire Leprince-Ringuet, CNRS/IN2P3, Ecole Polytechnique, Institut Polytechnique de Paris, Palaiseau, France*
[16]*LPNHE, Sorbonne Université, Paris Diderot Sorbonne Paris Cité, CNRS/IN2P3, Paris, France*
[17]*I. Physikalisches Institut, RWTH Aachen University, Aachen, Germany*
[18]*Universität Bonn—Helmholtz-Institut für Strahlen und Kernphysik, Bonn, Germany*
[19]*Fakultät Physik, Technische Universität Dortmund, Dortmund, Germany*
[20]*Physikalisches Institut, Albert-Ludwigs-Universität Freiburg, Freiburg, Germany*
[21]*Max-Planck-Institut für Kernphysik (MPIK), Heidelberg, Germany*
[22]*Physikalisches Institut, Ruprecht-Karls-Universität Heidelberg, Heidelberg, Germany*
[23]*School of Physics, University College Dublin, Dublin, Ireland*
[24]*INFN Sezione di Bari, Bari, Italy*
[25]*INFN Sezione di Bologna, Bologna, Italy*
[26]*INFN Sezione di Ferrara, Ferrara, Italy*
[27]*INFN Sezione di Firenze, Firenze, Italy*
[28]*INFN Laboratori Nazionali di Frascati, Frascati, Italy*
[29]*INFN Sezione di Genova, Genova, Italy*
[30]*INFN Sezione di Milano, Milano, Italy*
[31]*INFN Sezione di Milano-Bicocca, Milano, Italy*
[32]*INFN Sezione di Cagliari, Monserrato, Italy*
[33]*INFN Sezione di Padova, Padova, Italy*
[34]*INFN Sezione di Perugia, Perugia, Italy*
[35]*INFN Sezione di Pisa, Pisa, Italy*
[36]*INFN Sezione di Roma La Sapienza, Roma, Italy*
[37]*INFN Sezione di Roma Tor Vergata, Roma, Italy*
[38]*Nikhef National Institute for Subatomic Physics, Amsterdam, Netherlands*
[39]*Nikhef National Institute for Subatomic Physics and VU University Amsterdam, Amsterdam, Netherlands*
[40]*AGH—University of Krakow, Faculty of Physics and Applied Computer Science, Kraków, Poland*
[41]*Henryk Niewodniczanski Institute of Nuclear Physics Polish Academy of Sciences, Kraków, Poland*
[42]*National Center for Nuclear Research (NCBJ), Warsaw, Poland*
[43]*Horia Hulubei National Institute of Physics and Nuclear Engineering, Bucharest-Magurele, Romania*
[44]*Authors affiliated with an institute formerly covered by a cooperation agreement with CERN*
[45]*ICCUB, Universitat de Barcelona, Barcelona, Spain*

[46]*La Salle, Universitat Ramon Llull, Barcelona, Spain*
[47]*Instituto Galego de Física de Altas Enerxías (IGFAE), Universidade de Santiago de Compostela, Santiago de Compostela, Spain*
[48]*Instituto de Fisica Corpuscular, Centro Mixto Universidad de Valencia—CSIC, Valencia, Spain*
[49]*European Organization for Nuclear Research (CERN), Geneva, Switzerland*
[50]*Institute of Physics, Ecole Polytechnique Fédérale de Lausanne (EPFL), Lausanne, Switzerland*
[51]*Physik-Institut, Universität Zürich, Zürich, Switzerland*
[52]*NSC Kharkiv Institute of Physics and Technology (NSC KIPT), Kharkiv, Ukraine*
[53]*Institute for Nuclear Research of the National Academy of Sciences (KINR), Kyiv, Ukraine*
[54]*School of Physics and Astronomy, University of Birmingham, Birmingham, United Kingdom*
[55]*H.H. Wills Physics Laboratory, University of Bristol, Bristol, United Kingdom*
[56]*Cavendish Laboratory, University of Cambridge, Cambridge, United Kingdom*
[57]*Department of Physics, University of Warwick, Coventry, United Kingdom*
[58]*STFC Rutherford Appleton Laboratory, Didcot, United Kingdom*
[59]*School of Physics and Astronomy, University of Edinburgh, Edinburgh, United Kingdom*
[60]*School of Physics and Astronomy, University of Glasgow, Glasgow, United Kingdom*
[61]*Oliver Lodge Laboratory, University of Liverpool, Liverpool, United Kingdom*
[62]*Imperial College London, London, United Kingdom*
[63]*Department of Physics and Astronomy, University of Manchester, Manchester, United Kingdom*
[64]*Department of Physics, University of Oxford, Oxford, United Kingdom*
[65]*Massachusetts Institute of Technology, Cambridge, Massachusetts, USA*
[66]*University of Cincinnati, Cincinnati, Ohio, USA*
[67]*University of Maryland, College Park, Maryland, USA*
[68]*Los Alamos National Laboratory (LANL), Los Alamos, New Mexico, USA*
[69]*Syracuse University, Syracuse, New York, USA*
[70]*Pontifícia Universidade Católica do Rio de Janeiro (PUC-Rio), Rio de Janeiro, Brazil (associated with Universidade Federal do Rio de Janeiro (UFRJ), Rio de Janeiro, Brazil)*
[71]*Universidad Andres Bello, Santiago, Chile (associated with Physik-Institut, Universität Zürich, Zürich, Switzerland)*
[72]*School of Physics and Electronics, Hunan University, Changsha City, China (associated with Institute of Particle Physics, Central China Normal University, Wuhan, Hubei, China)*
[73]*Guangdong Provincial Key Laboratory of Nuclear Science, Guangdong-Hong Kong Joint Laboratory of Quantum Matter, Institute of Quantum Matter, South China Normal University, Guangzhou, China (associated with Department of Engineering Physics, Tsinghua University, Beijing, China)*
[74]*Lanzhou University, Lanzhou, China (associated with Institute Of High Energy Physics (IHEP), Beijing, China)*
[75]*School of Physics and Technology, Wuhan University, Wuhan, China (associated with Department of Engineering Physics, Tsinghua University, Beijing, China)*
[76]*Henan Normal University, Xinxiang, China (associated with Institute of Particle Physics, Central China Normal University, Wuhan, Hubei, China)*
[77]*Departamento de Fisica, Universidad Nacional de Colombia, Bogota, Colombia (associated with LPNHE, Sorbonne Université, Paris Diderot Sorbonne Paris Cité, CNRS/IN2P3, Paris, France)*
[78]*Ruhr Universitaet Bochum, Fakultaet f. Physik und Astronomie, Bochum, Germany (associated with Fakultät Physik, Technische Universität Dortmund, Dortmund, Germany)*
[79]*Eotvos Lorand University, Budapest, Hungary (associated with European Organization for Nuclear Research (CERN), Geneva, Switzerland)*
[80]*Faculty of Physics, Vilnius University, Vilnius, Lithuania (associated with Physikalisches Institut, Albert-Ludwigs-Universität Freiburg, Freiburg, Germany)*
[81]*Van Swinderen Institute, University of Groningen, Groningen, Netherlands (associated with Nikhef National Institute for Subatomic Physics, Amsterdam, Netherlands)*
[82]*Universiteit Maastricht, Maastricht, Netherlands (associated with Nikhef National Institute for Subatomic Physics, Amsterdam, Netherlands)*
[83]*Tadeusz Kosciuszko Cracow University of Technology, Cracow, Poland (associated with Henryk Niewodniczanski Institute of Nuclear Physics Polish Academy of Sciences, Kraków, Poland)*
[84]*Universidade da Coruña, A Coruña, Spain (associated with La Salle, Universitat Ramon Llull, Barcelona, Spain)*
[85]*Department of Physics and Astronomy, Uppsala University, Uppsala, Sweden (associated with School of Physics and Astronomy, University of Glasgow, Glasgow, United Kingdom)*
[86]*Taras Schevchenko University of Kyiv, Faculty of Physics, Kyiv, Ukraine (associated with Université Paris-Saclay, CNRS/IN2P3, IJCLab, Orsay, France)*

[87]University of Michigan, Ann Arbor, MI, United States (associated with Syracuse University, Syracuse, New York, USA)
[88]Ohio State University, Columbus, United States (associated with Los Alamos National Laboratory (LANL), Los Alamos, New Mexico, USA)

[a]Deceased.
[b]Also at Lamarr Institute for Machine Learning and Artificial Intelligence, Dortmund, Germany.
[c]Also at Università degli Studi di Milano-Bicocca, Milano, Italy.
[d]Also at Università di Roma Tor Vergata, Roma, Italy.
[e]Also at Università di Modena e Reggio Emilia, Modena, Italy.
[f]Also at Department of Physics and Astronomy, University of Victoria, Victoria, Canada.
[g]Also at Università di Ferrara, Ferrara, Italy.
[h]Also at Universidade Estadual de Campinas (UNICAMP), Campinas, Brazil.
[i]Also at Università di Bologna, Bologna, Italy.
[j]Also at Università di Genova, Genova, Italy.
[k]Also at Scuola Normale Superiore, Pisa, Italy.
[l]Also at Università degli Studi di Milano, Milano, Italy.
[m]Also at Center for High Energy Physics, Tsinghua University, Beijing, China.
[n]Also at Universidad Nacional Autónoma de Honduras, Tegucigalpa, Honduras.
[o]Also at Università di Cagliari, Cagliari, Italy.
[p]Also at Centro Federal de Educacão Tecnológica Celso Suckow da Fonseca, Rio De Janeiro, Brazil.
[q]Also at Università di Bari, Bari, Italy.
[r]Also at Università di Perugia, Perugia, Italy.
[s]Also at Università di Padova, Padova, Italy.
[t]Also at LIP6, Sorbonne Université, Paris, France.
[u]Also at Università di Pisa, Pisa, Italy.
[v]Also at Hangzhou Institute for Advanced Study, UCAS, Hangzhou, China.
[w]Also at Università di Bergamo, Bergamo, Italy.
[x]Also at Universidad de Ingeniería y Tecnología (UTEC), Lima, Peru.
[y]Also at Università di Siena, Siena, Italy.
[z]Also at Università della Basilicata, Potenza, Italy.
[aa]Also at Universidad de Alcalá, Alcalá de Henares, Spain.
[bb]Also at Università di Urbino, Urbino, Italy.